

# On the Energetic Dependence of Charge Separation in Low-Band-Gap Polymer/Fullerene Blends

Stoichko D. Dimitrov,<sup>†</sup> Artem A. Bakulin,<sup>‡,§</sup> Christian B. Nielsen,<sup>†</sup> Bob C. Schroeder,<sup>†</sup> Junping Du,<sup>†</sup> Hugo Bronstein,<sup>†</sup> Iain McCulloch,<sup>†</sup> Richard H. Friend,<sup>‡</sup> and James R. Durrant<sup>\*,†</sup>

<sup>†</sup>Centre for Plastic Electronics, Department of Chemistry, Imperial College London, Exhibition Road, London SW7 2AZ, United Kingdom

<sup>‡</sup>Cavendish Laboratory, University of Cambridge, Cambridge CB3 0HE, United Kingdom

**S** Supporting Information

**ABSTRACT:** The energetic driving force required to drive charge separation across donor/acceptor heterojunctions is a key consideration for organic optoelectronic devices. Herein we report a series of transient absorption and photocurrent experiments as a function of excitation wavelength and temperature for two low-band-gap polymer/fullerene blends to study the mechanism of charge separation at the donor/acceptor interface. For the blend that exhibits the smallest donor/acceptor LUMO energy level offset, the photocurrent quantum yield falls as the photon excitation energy is reduced toward the band gap, but the yield of bound, interfacial charge transfer states rises. This interplay between bound and free charge generation as a function of initial exciton energy provides key evidence for the role of excess energy in driving charge separation of direct relevance to the development of low-band-gap polymers for enhanced solar light harvesting.

Charge separation and recombination at organic donor/acceptor (D/A) heterojunctions is a key factor in the successful design of organic optoelectronic devices, including light-emitting diodes and solar cells.<sup>1–3</sup> Minimizing the energy offset required to drive charge separation at this interface is a key consideration for optimizing the thermodynamic efficiency of such devices, including in particular the utilization of new donor polymers with lower optical band gaps and therefore improved harvesting of solar irradiation.<sup>4–6</sup> Semiconducting organic materials typically have dielectric constants of  $\sim 3$ . These low dielectric constants cannot screen the electrostatic interactions between opposing charges across the D/A interface, which can result in the formation of interfacial bound electron–hole (e–h) pairs. Often called charge transfer (CT) states, these e–h pairs have binding energies  $\sim 1$  order of magnitude higher than  $k_B T$ .<sup>7</sup> Understanding what determines whether these interfacial states dissociate to form free charges is a key unresolved challenge for such organic optoelectronic devices.

Most models of charge photogeneration in organic materials derive from the Onsager theory of charge separation, which predicts the escape probability of photogenerated Coulombically bound e–h pairs from the laws of Brownian motion.<sup>7,8</sup> Building upon Onsager theory, Morteani et al.<sup>9</sup> and Peumans and Forrest<sup>10</sup> proposed that excess energy is an important

factor in overcoming the electrostatic e–h attraction of the bound charges. Two types of CT states were identified; relaxed CT states that predominantly recombine to the ground state and hot CT states with enough excess energy to drive efficient charge dissociation. We note that these hot CT states may correspond to different electronic states and/or states with higher degrees of delocalization.<sup>11–13</sup> The importance of excess energy was later supported by Ohkita et al.,<sup>14</sup> who studied a series of polythiophene polymer/fullerene blends and showed that while the exciton separation was efficient for all the blends studied, the yield of dissociated charges correlated with the magnitude of the energy offset driving the charge separation. This was assigned to hot CT states being required to drive charge dissociation.<sup>14,15</sup> However, experimental evidence against the importance of large excess energy for charge separation has also been provided.<sup>16–18</sup> For example, Lee et al.<sup>16</sup> used direct photocurrent spectroscopy to compare the device photocurrents in polymer/PCBM blends with a rather large energy offset for below- and above-band-gap excitations; they concluded that charge generation in polymer/fullerene blends does not require large excess energy but rather that the directly photogenerated CT state could undergo charge dissociation. More recently, it was demonstrated that polaronic relaxation of such directly photogenerated CT states brings about CT localization.<sup>13</sup>

Here we report a study of charge photogeneration as a function of excitation wavelength in two low-band-gap polymer/fullerene bulk heterojunctions with relatively small material energy offsets. Our studies employed both transient optical studies of polaron yields and innovative pump–push studies of CT state dissociation to show that for systems with low driving energy for charge separation, the amount of excess energy injected into the CT state determines the final yield of free charges.

Figure 1a displays the chemical structure of the polymer used in this study, BTT-DPP, a low-band-gap polymer that has a high hole mobility but exhibits relatively inefficient charge generation from polymer excitons when blended with the widely used fullerene acceptor [6,6]-phenyl-C61-butyric acid methyl ester (PCBM).<sup>19</sup> BTT-DPP/PCBM has no offset or driving energy for charge separation:  $\Delta E_{\text{CSeff}} \approx 0.0$  eV, where

Received: August 21, 2012

Published: October 24, 2012

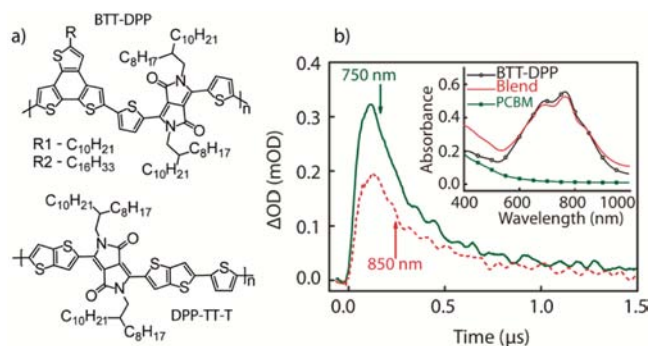


**Figure 1.** (a) Chemical structures of BTT-DPP and DPP-TT-T. Two different batches of BTT-DPP with different side chains were used for the pump–push photocurrent spectroscopy and TAS experiments. Details of the polymer syntheses are included in the SI. (b) Transient absorption decays at 750 and 850 nm. Inset: steady-state absorption spectra of thin films of BTT-DPP, PCBM, and a 1:1 BTT-DPP/PCBM blend.

$\Delta E_{\text{CS}_{\text{eff}}} = \text{SE} - (\text{IP}_{\text{D}} - \text{EA}_{\text{A}})$ , in which SE is the lowest energy polymer singlet exciton,  $\text{IP}_{\text{D}}$  is the ionization potential of the donor and  $\text{EA}_{\text{A}}$  is the electron affinity of the acceptor.<sup>20</sup> This D/A pair was chosen because of its low  $\Delta E_{\text{CS}_{\text{eff}}}$  and poor charge generation properties, which make it a good candidate for use in investigating any possible excitation wavelength dependence of charge generation. A reference blend employed an analogous low-band-gap polymer, DPP-TT-T (Figure 1a).<sup>6</sup> DPP-TT-T/PCBM has  $\Delta E_{\text{CS}_{\text{eff}}} \approx 0.15$  eV and exhibits relatively efficient photocurrent generation, consistent with the larger energy offset favoring efficient charge dissociation, in agreement with our previous studies.<sup>13,14</sup>

We employed transient absorption spectroscopy (TAS) on the nano- to microsecond time scale to estimate the yield of photogenerated charges as a function of excitation wavelength and temperature.<sup>15,21</sup> For the BTT-DPP/PCBM blend, we first identified the maximum absorption of the positive polymer polaron to be at 1200 nm [Figure S3 in the Supporting Information (SI)]. The decay dynamics of this polaron absorption signal fitted well to a single power law decay ( $\Delta\text{OD} \propto t^{-\alpha}$ ), characteristic of diffusion-limited nongeminate recombination of trapped dissociated polarons.<sup>14</sup> We did not observe a change in the exponent  $\alpha$  with excitation wavelength. The negative PCBM polaron absorbs at 1050 nm with a low extinction coefficient. Therefore, the amplitude of the 1200 nm band reflects the photoinduced polaron concentration in the studied blends.

To explore the effect of excitation photon energy on charge separation, we recorded the amplitude of the transient absorption signal at 0.2  $\mu\text{s}$  as a function of excitation wavelength and thus constructed a transient-absorption excitation spectrum (TES). The TES of the BTT-DPP/PCBM blend (Figure 2) reveals that the quantum yield of charges was dependent on the wavelength of the excitation pulses. Notably, as the excitation wavelength was extended beyond 750 nm, the yield of photogenerated charges per absorbed photon was reduced. This is also visible in Figure 1b, in which the  $\Delta\text{OD}$  transients for 750 and 850 nm excitation are plotted. This TES was compared to the photocurrent internal quantum efficiency (IQE) of a corresponding BTT-DPP/PCBM photovoltaic (PV) device (determined without correcting for optical interference effects). A good match between the TES and IQE spectrum was observed, consistent

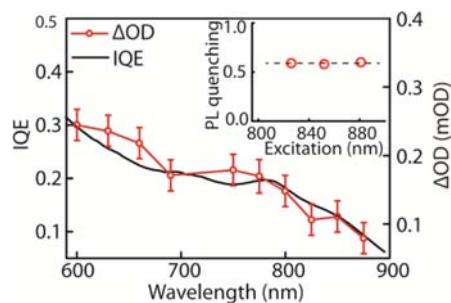


**Figure 2.** TES of a BTT-DPP/PCBM blend recorded at the polymer polaron band (1150 nm) at a 0.2  $\mu\text{s}$  time delay (red  $\circ$ ). Error bars represent one standard deviation combined with the scaling uncertainty. The TES and the IQE of the corresponding device (black line) show similar increases in the charge yield with excitation wavelength. Inset: PL quenching of the BTT-DPP/PCBM blend plotted as a function of excitation wavelength.

with our previous studies showing a close correlation between our transient absorption assay of charge generation and the device photocurrent density.<sup>19,22</sup> We note that for wavelengths  $>650$  nm, PCBM absorption in the BTT-DPP/PCBM blend was negligible ( $<0.3\%$ ; Figure 1b inset). Therefore, the observed excitation wavelength dependence of charge photo-generation and photocurrent IQE between 650 and 900 nm can be assigned to the excitation of polymer excitons with different initial energies. In contrast to the BTT-DPP/PCBM blend, the control TES for the DPP-TT-T/PCBM blend showed no dependence upon excitation wavelength (Figure S4), consistent with the blend's larger  $\Delta E_{\text{CS}_{\text{eff}}}$  enabling efficient charge generation for this blend.

The TES and IQE data in Figure 2 demonstrate that the efficiency of charge generation can depend upon the energy of the photoexcited polymer excitons, with excitons generated at the band edge yielding fewer charges than excitons above the band edge. This property of the BTT-DPP/PCBM blend could derive from an excitation wavelength dependence of the exciton quenching. However, the results from photoluminescence (PL) quenching experiments (Figure 2 inset) indicate that quenching of the BTT-DPP singlet excitons is independent of excitation wavelength, which suggests that the efficiency of free charge generation is not determined by the exciton dissociation yields in this system.

To elucidate further the dynamics of charge separation and bound CT state formation, we applied a novel ultrafast pump–push photocurrent technique (Figure S6).<sup>13,23</sup> In the experiment, a BTT-DPP/PCBM PV device is first exposed to a 200 fs visible-light “pump” pulse. After a certain delay time, the PV device is illuminated with a 250 fs IR (2200 nm) push pulse. The push pulse is selectively absorbed by the hole polarons, as the neutral polymer chains are transparent in this spectral region while the polymer polarons typically exhibit a strong absorption at this wavelength.<sup>24</sup> The IR push pulse provides these hole polarons with excess energy, bringing them to an otherwise energetically inaccessible hot state. Therefore, bound charge pairs generated at the organic interface by the visible-light pump pulse can potentially be converted to free charge carriers with the help of the excess energy provided by the IR push pulse. In the experiment, we detect the effect of the push pulse by monitoring the relative increase of the photocurrent output ( $\delta J/J$ ) of the PV device. We note that free positive polarons contribute to the photocurrent  $J$  without the push pulse and thus do not affect the experimentally observable  $\delta J/J$ ,

making the experiment selective solely for the ratio of bound and free polaron states generated by the pump pulse.

Figure 3 shows the changes in the photocurrent due to the pump pulse as a function of pump–push delay for the BTT-

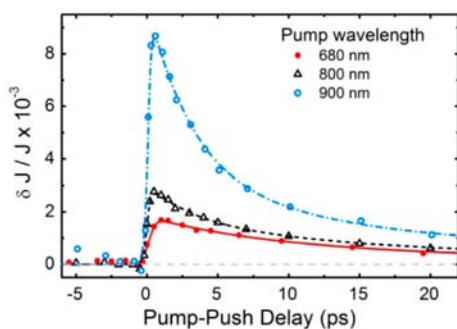


**Figure 3.** Results of pump–push photocurrent ( $\delta J/J$ ) measurements on BTT-DPP/PCBM devices at different excitation wavelengths. Lines are exponential fits convoluted with the 200 fs response function.

DPP/PCBM PV device excited at different pump wavelengths. In all of these experiments, when the push pulse arrived before the pump pulse, the effect on  $\delta J/J$  was negligible because there were very few charges in the cell to be influenced by the IR photons. When the push arrived after the pump pulse,  $\delta J/J$  increased for all of the PV devices. This is direct evidence of the existence of bound charge pairs at the D/A interface. The sharp increase in signal was dominated by a prompt component, demonstrating that the majority of bound polarons are generated on an ultrafast time scale. Interestingly, as the energy of the pump photon was decreased from 1.80 eV (680 nm) to 1.38 eV (900 nm), the amplitude of the  $\delta J/J$  response increased dramatically. This provides direct evidence that the amount of bound charges increased (by a factor of  $\geq 2$ ) as the amount of excess energy initially put into the exciton decreased. This result is in qualitative and quantitative agreement with IQE and TES spectra. More importantly, the increase in the yield of bound charges with the pump wavelength indicates that the variations in the IQE and charge yields originated not from inefficient exciton dissociation but rather from increased charge trapping in bound, relaxed interfacial CT states that are unable to dissociate efficiently. Another conclusion that may be drawn from the pump–push photocurrent experiments is based on the observation that bound states were formed very fast, within  $\sim 1$  ps after excitation. The absence of a growing component in the transients signifies that charge separation was not preceded by an extensive exciton migration and occurred locally.<sup>25</sup> However, much slower diffusion-limited processes may also be present for a subensemble of excitonic states as a result of possible different morphology configurations in the blends, but these were not resolved in our experiment.

It is important to consider the role of inhomogeneity in the donor polymer. Though the absorption spectrum in Figure 1 shows evidence for vibronic structure, this is not particularly well developed, and the long-wavelength tail of the absorption is relatively shallow; both of these indicate that there is a distribution of local  $\pi$ - $\pi^*$  polymer band gaps associated with different local chain configurations. Thus, the local driving energy for charge separation varies, being larger for higher-band-gap regions of the polymer. Therefore, excitation at different wavelengths in IQE, TES, or pump–push photocurrent experiments both controls the excess energy above the

vibrationally relaxed exciton and also can target different subensembles of heterojunctions with different electronic structures.

To explain the observed excitation-wavelength-dependent charge generation in the BTT-DPP blend, we propose the qualitative model of charge generation illustrated in Figure 4.<sup>1,2</sup>

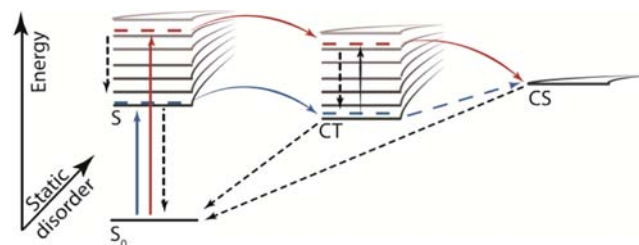


**Figure 4.** Energy level diagram depicting two charge separation processes initiated by light excitations using photons with high energy (red arrows) and low energy (blue arrows).

In this model, photon-to-charge conversion is realized by evolution through three state manifolds: singlet excitons (S), CT states, and separated charges (CS). We assume that possible variations in the local morphologies also create a distribution of the manifold energies, which causes broadening of the absorption spectrum. During the charge separation, electron transfer from the polymer to the fullerene competes successfully with other nonradiative reaction pathways for exciton relaxation, such as thermal relaxation or internal conversion of the excitons to the bottom of the exciton band.<sup>26–28</sup> In this case, all of the photogenerated excitons, irrespective of their energy, can dissociate at the D/A interface and translate their excess energy to the CT state. This ultrafast reaction therefore generates different vibrational or electronic CT states with different excess energies. Both relatively hot and relatively relaxed CT states will be populated, depending on the energy of the exciting photons and the local morphology/energy level structure. However, the efficiency of dissociation of these CT states into free charges is dependent upon the amount of excess energy of the initially generated CT states.

The model presented in Figure 4 illustrates the concept that relaxed CT states and hot CT states with insufficiently high driving energy cannot undergo efficient charge dissociation. This concept is consistent with the notion that these interfacial CT states exhibit a significant Coulomb binding energy and the proposal that efficient charge dissociation proceeds only from unrelaxed or hot CT states. To examine this issue further, we undertook additional tests of the charge photogeneration properties of the BTT-DPP and DPP-TT-T blends as a function of temperature. The results for both polymer/PCBM blends (Figure S5) showed temperature-independent charge generation between 110 and 300 K, in agreement with the results of previous studies of charge separation in polymer/fullerene blends.<sup>29,30</sup> This suggests that charge dissociation in both of these blends is not a thermally activated process. Another conclusion that can be derived from the absence of a temperature dependence is that charges in the relaxed CT state are strongly trapped.

Previous studies of charge photogeneration as a function of excitation wavelength in polymer/fullerene blends have typically compared the response of blends to photoexcitations at or below the polymer band gap.<sup>12,16,18</sup> Such studies have focused on blends such as P3HT:PCBM, where band-gap



excitation results in efficient charge generation, and have observed that photoexcitation below this band gap into a weak absorption tail assigned to direct excitation of CT states can also result in efficient charge generation. In the present study, we have taken a different approach, employing a low-band-gap polymer where the small LUMO level offset results in band-gap excitation generating only a relatively low yield of charges. This has allowed us to investigate whether above-band-gap photoexcitation into strongly allowed optical transitions of the polymer results in enhanced charge generation. Our study has therefore avoided the difficulties associated with interpretation of data from excitation of optical transitions with very low oscillator strengths and is moreover of direct relevance to technology drives to utilize lower-band-gap polymers to enhance solar light absorption.<sup>4–6</sup>

In summary, we have performed a detailed study of the mechanism of charge photogeneration in a model organic D/A system with a relatively small driving force for charge separation. The charge photogeneration behavior of the blend film was found to be strongly dependent upon the photon energy used to generate the polymer excitons. Specifically, increasing this photon energy by  $\sim 0.2$  eV above the optical band gap was observed to double the quantum yield of dissociated charges and the device photocurrent IQE, correlated with a substantial decrease in the yield of relaxed, bound interfacial CT states. These data strongly support a model wherein charge dissociation is dependent upon having the excess energy of initially generated hot CT states overcome their Coulomb attraction. The particular mechanism of this dissociation probably involves a relatively high level of delocalization of hot CT states.<sup>13</sup> These results thus provide new insight into the energy offsets required to drive charge dissociation at organic D/A interfaces, which comprise the ultimate limits to the efficiencies achievable with organic PV heterojunctions.

## ■ ASSOCIATED CONTENT

### ■ Supporting Information

Synthesis of monomers and the BTT-DPP copolymer, <sup>1</sup>H NMR spectra, details of film and device preparation, TAS and pump–push photocurrent spectroscopy results, PL spectra, and complete refs 6 and 14. This material is available free of charge via the Internet at <http://pubs.acs.org>.

## ■ AUTHOR INFORMATION

### Corresponding Author

[j.durrant@imperial.ac.uk](mailto:j.durrant@imperial.ac.uk)

### Present Address

<sup>§</sup>FOM institute AMOLF, Science Park 104, Amsterdam, The Netherlands

### Notes

The authors declare no competing financial interest.

## ■ ACKNOWLEDGMENTS

We thank the EPSRC for financial support, L. Hirst and M. Fuhrer for their help with the electroluminescence setup, P. Shakya and N. Tokmoldin for assistance with device fabrication, and S. E. Watkins (CSIRO Materials Science and Engineering, VIC 3169, Victoria, Australia) for IP measurements. A.A.B. acknowledges a VENI Grant from The Netherlands Organization for Scientific Research (NWO)

## ■ REFERENCES

- (1) Clarke, T. M.; Durrant, J. R. *Chem. Rev.* **2010**, *110*, 6736.
- (2) Brédas, J.-L.; Norton, J. E.; Cornil, J.; Coropceanu, V. *Acc. Chem. Res.* **2009**, *42*, 1691.
- (3) Zhu, X. Y.; Yang, Q.; Muntwiler, M. *Acc. Chem. Res.* **2009**, *42*, 1779.
- (4) Mühlbacher, D.; Scharber, M.; Morana, M.; Zhu, Z.; Waller, D.; Gaudiana, R.; Brabec, C. *Adv. Mater.* **2006**, *18*, 2884.
- (5) Park, S. H.; Roy, A.; Beaupre, S.; Cho, S.; Coates, N.; Moon, J. S.; Moses, D.; Leclerc, M.; Lee, K.; Heeger, A. J. *Nat. Photonics* **2009**, *3*, 297.
- (6) Bronstein, H.; et al. *J. Am. Chem. Soc.* **2011**, *133*, 3272.
- (7) Deibel, C.; Strobel, T.; Dyakonov, V. *Adv. Mater.* **2010**, *22*, 4097.
- (8) Onsager, L. *Phys. Rev.* **1938**, *54*, 554.
- (9) Morteani, A. C.; Sreearunothai, P.; Herz, L. M.; Friend, R. H.; Silva, C. *Phys. Rev. Lett.* **2004**, *92*, No. 247402.
- (10) Peumans, P.; Forrest, S. R. *Chem. Phys. Lett.* **2004**, *398*, 27.
- (11) Scharber, M. C.; Lungenschmied, C.; Egelhaaf, H.-J.; Matt, G.; Bednorz, M.; Fromherz, T.; Gao, J.; Jarzab, D.; Loi, M. A. *Energy Environ. Sci.* **2011**, *4*, 5077.
- (12) Murthy, D. H. K.; Gao, M.; Vermeulen, M. J. W.; Siebbeles, L. D. A.; Savenije, T. J. *J. Phys. Chem. C* **2012**, *116*, 9214.
- (13) Bakulin, A. A.; Rao, A.; Pavelyev, V. G.; van Loosdrecht, P. H. M.; Pshenichnikov, M. S.; Niedzialek, D.; Cornil, J.; Beljonne, D.; Friend, R. H. *Science* **2012**, *335*, 1340.
- (14) Ohkita, H.; et al. *J. Am. Chem. Soc.* **2008**, *130*, 3030.
- (15) Shoaee, S.; Clarke, T. M.; Huang, C.; Barlow, S.; Marder, S. R.; Heeney, M.; McCulloch, I.; Durrant, J. R. *J. Am. Chem. Soc.* **2010**, *132*, 12919.
- (16) Lee, J.; Vandewal, K.; Yost, S. R.; Bahlke, M. E.; Goris, L.; Baldo, M. A.; Manca, J. V.; Van Voorhis, T. *J. Am. Chem. Soc.* **2010**, *132*, 11878.
- (17) Zhou, Y.; Tvingstedt, K.; Zhang, F.; Du, C.; Ni, W.-X.; Andersson, M. R.; Inganäs, O. *Adv. Funct. Mater.* **2009**, *19*, 3293.
- (18) van der Hofstad, T. G. J.; Di Nuzzo, D.; van den Berg, M.; Janssen, R. A. J.; Meskers, S. C. J. *Adv. Energy Mater.* **2012**, *2*, 1095.
- (19) Dimitrov, S. D.; Nielsen, C. B.; Shoaee, S.; Tuladhar, P. S.; Du, J.; McCulloch, I.; Durrant, J. R. *J. Phys. Chem. Lett.* **2012**, *3*, 140.
- (20) Coffey, D. C.; Larson, B. W.; Hains, A. W.; Whitaker, J. B.; Kopidakis, N.; Boltalina, O. V.; Strauss, S. H.; Rumbles, G. *J. Phys. Chem. C* **2012**, *116*, 8916.
- (21) Etzold, F.; Howard, I. A.; Mauer, R.; Meister, M.; Kim, T. D.; Lee, K. S.; Baek, N. S.; Laquai, F. *J. Am. Chem. Soc.* **2011**, *133*, 9469.
- (22) Clarke, T. M.; Ballantyne, A.; Shoaee, S.; Soon, Y. W.; Duffy, W.; Heeney, M.; McCulloch, I.; Nelson, J.; Durrant, J. R. *Adv. Mater.* **2010**, *22*, 5287.
- (23) Muller, J. G.; Lemmer, U.; Feldmann, J.; Scherf, U. *Phys. Rev. Lett.* **2002**, *88*, No. 147401.
- (24) Sheng, C. X.; Tong, M.; Singh, S.; Vardeny, Z. V. *Phys. Rev. B* **2007**, *75*, No. 085206.
- (25) Vaynzof, Y.; Bakulin, A. A.; Gelinis, S.; Friend, R. H. *Phys. Rev. Lett.* **2012**, *108*, No. 246605.
- (26) Tong, M.; Coates, N. E.; Moses, D.; Heeger, A. J.; Beaupre, S.; Leclerc, M. *Phys. Rev. B* **2010**, *81*, No. 125210.
- (27) Howard, I. A.; Mauer, R.; Meister, M.; Laquai, F. *J. Am. Chem. Soc.* **2010**, *132*, 14866.
- (28) Katz, G.; Ratner, M. A.; Kosloff, R. *J. Phys. Chem. A* **2011**, *115*, 5833.
- (29) Grzegorzczak, W. J.; Savenije, T. J.; Dykstra, T. E.; Pirus, J.; Schins, J. M.; Siebbeles, L. D. A. *J. Phys. Chem. C* **2010**, *114*, 5182.
- (30) Pensack, R. D.; Banyas, K. M.; Asbury, J. B. *J. Phys. Chem. B* **2010**, *114*, 12242.